Published online January 12, 2005

190–200 *Nucleic Acids Research, 2005, Vol. 33, No. 1*
doi:10.1093/nar/gki153

The RNA ligands for mouse proline-rich RNA-binding protein (mouse Prrp) contain two consensus sequences in separate loop structure

Tamaki Hori, Yusuke Taguchi, Seiichi Uesugi and Yasuyuki Kurihara*

Department of Environment and Natural Sciences, Graduate School of Environment and Information Sciences, Yokohama National University, Tokiwa-dai, Hodogaya, Yokohama 240-0851, Japan

Received November 4, 2004; Revised and Accepted December 8, 2004

ABSTRACT

Mouse proline-rich RNA-binding protein (mPrrp) is a mouse ortholog of *Xenopus* Prrp, which binds to a vegetal localization element (VLE) in the 3′-untranslated region (3′-UTR) of Vg1 mRNA and is expected to be involved in the transport and/or localization of Vg1 mRNA to the vegetal cortex of oocytes. In mouse testis, mPrrp protein is abundantly expressed in the nuclei of pachytene spermatocytes and round spermatids, and shifts to the cytoplasm in elongating spermatids. To gain an insight into the function of mPrrp in male germ cells, we performed *in vitro* RNA selection (SELEX) to determine the RNA ligand sequence of mPrrp. This analysis revealed that many of the selected clones contained both of two conserved elements, AAAUAG and $GU_{1-3}AG$. RNA-binding study on deletion mutants and secondary structure analyses of the selected RNA revealed that a two-loop structure containing the conserved elements is required for high-affinity binding to mPrrp. Furthermore, we found that the target mRNAs of *Xenopus* Prrp contain intact AAAUAG and $GU_{1-3}AG$ sequences in the 3′-UTR, suggesting that these binding sequences are shared by Prrps of *Xenopus* and mouse.

INTRODUCTION

Spermatogenesis is a process by which immature male germ cells go through a complex series of differentiation steps involving mitotic and meiotic cell divisions and morphogenesis, which finally lead to the formation of mature spermatozoa. These multiple differentiation steps appear to rely on complex regulation of time- and region-specific expression of genetic information (1). In particular, haploid germ cell differentiation after meiotic division, which is also known as spermiogenesis, is mainly regulated at the post-transcriptional level (2). During this time period, the cell cycle of haploid spermatids is arrested, the chromatin in the nucleus condenses and transcriptional activity begins to slow, ceasing completely during later spermiogenesis. However, spermatids undergo many drastic morphological differentiations, which involve nuclear condensation, elimination of most of the spermatid cytoplasm, and formation of the tail and acrosome. These processes require the synthesis of *de novo* proteins, and a few of these proteins are derived from stored mRNA transcribed earlier in the spermatocyte nucleus. Such translational regulation is mediated by specific proteins that bind RNA and continue being translated in the absence of transcription (1). Therefore, RNA-binding proteins may play important roles in spermatogenesis.

Mouse proline-rich RNA-binding protein (mPrrp), otherwise known as DAZAP1, is an RNA-binding protein that is abundantly expressed in male germ cells (3). The protein is evolutionarily highly conserved from *Xenopus* (xPrrp) (4) to human (3). xPrrp was identified as one of the proteins that bind to VLE of Vg1 mRNA (4). VLE is a 340-nt *cis* control element that transports and anchors Vg1 mRNA to the vegetal pole in *Xenopus* oocytes, indicating that xPrrp may be involved in the transport/localization of Vg1 mRNA (4,5). Immunohistochemical analysis of the mouse protein revealed stage-specific changes in subcellular localization during spermatogenesis [(6); Y. Kurihara, unpublished data]. mPrrp is abundantly expressed in the nuclei of late pachytene spermatocytes and round spermatids, and is redistributed to the cytoplasm in elongating spermatids. Among RNA-binding proteins, a stage-specific change in subcellular localization has been reported for TB-RBP (7), which is involved in mRNA transport in male germ and neuronal cells. Although the biological significance of the stage-specific shift is not known, we assume that mPrrp is involved in stage-specific mRNA transport, as in the case of xPrrp.

*To whom correspondence should be addressed. Tel/Fax: +81 45 339 4263; Email: kurihara@mac.bio.bsk.ynu.ac.jp

To gain an insight into the function of mPrrp in male germ cells, it is essential to identify the target mRNA that is regulated by mPrrp. Determination of the RNA-binding specificity of mPrrp will certainly provide an important clue for identifying the target RNAs and for elucidating the function of mPrrp in mammalian spermatogenesis. In this study, we used the *in vitro* RNA selection method to identify the RNA sequence required for binding to mPrrp. We found two consensus sequences, AAAUAG and $GU_{1-3}AG$, in the selected RNA ligands, and secondary structure analysis showed that two loop structures each containing one individual consensus sequence are important for high-affinity binding to mPrrp. Since the conserved sequences, AAAUAG and $GU_{1-3}AG$, are also found in the 3′-UTR of the all known target mRNAs of *Xenopus* Prrp, these two sequences may be the common sequences recognized by the Prrp family.

MATERIALS AND METHODS

Thioredoxin- and His_6-tagged mPrrp constructs

Mouse Prrp cDNAs were prepared by RT–PCR. Total RNA was isolated from adult mouse testis using TRI® Reagent (Sigma). To obtain full-length mPrrp (mPrrp-FL: 1–405 amino acids), the RNA was reverse transcribed using Sensiscript reverse transcriptase (QIAGEN), and the first-strand cDNA was amplified with *PfuTurbo* DNA polymerase (Stratagene) using the following primers: forward primer, 5′-CCG GCC ATG GCT AAC AGC GCG GGC GCC GAC G-3′; reverse primer, 5′-AGA AGC GGC CGC GCG CCG GTA GGG ATG GAA-3′. The cDNA was introduced into the NcoI/NotI sites of the pET32(a) expression vector (Novagen) to produce thioredoxin and polyhistidine fusion proteins. For preparation of the two RNA-binding domains and the proline-rich region of mPrrp, cDNAs were obtained by PCR amplification from mPrrp-FL cDNA as the template using the following primers. Two RNA-binding domains (mPrrp-2xRBD: 1–201 amino acids): forward primer, 5′-CCG GCC ATG GCT AAC AGC GCG GGC GCC GAC G-3′; reverse primer, 5′-AGA AGC GGC CGC GCG CCG GTA GGG ATG GAA-3′. Proline-rich region of mPrrp (mPrrp-Pro: 200–405 amino aicds): forward primer, 5′-GAA AGG ATC CCA GCC AGG AGC CAG CCA G-3′; reverse primer, 5′-AGA AGC GGC CGC GCG CCG GTA GGG ATG GAA-3′. These cDNAs were introduced into the NcoI/NotI or BamHI/NotI sites of the pET32(a) expression vector. The plasmid was transformed into *Escherichia coli* BL21(DE3)RP. The expression and affinity purification of these fusion mPrrp proteins were performed according to the manufacturer's instructions.

In vitro RNA selection

RNA selection was performed according to the method described by others with minor modifications (8,9). Oligonucleotides harboring a 50-bp random sequence flanked by primer binding sites (5′-GGG AAG ATC TCG ACC AGA AG N50 TAT GTG CGT CTA CAT GGA TCC TCA-3′) were synthesized using a DNA synthesizer (ABI 391 DNA Synthesizer, ABI). About 1 nmol of this oligonucleotide was amplified by PCR using a forward primer containing the T7 promoter sequence (SEL-FR, 5′-CGG AAT TCT AAT ACG ACT CAC TAT AGG GAA GAT CTC GAC CAG AAG-3′) and a reverse primer (SEL-RV, 5′-TGA GGA TCC ATG TAG ACG CAC ATA-3′) under the following conditions: 10 cycles of 30 s at 94°C, 30 s at 59°C, 5 s at 72°C. A 30 µg of these library DNAs were transcribed *in vitro* with T7 RNA polymerase according to the procedure of Tanaka *et al*. (10), and the transcribed RNA was purified by 8% denaturing polyacrylamide gel electrophoresis. The purified RNA was heat-denatured at 95°C for 1 min, and preabsorbed with Ni-NTA Agarose Resin (QIAGEN) to remove nonspecifically bound RNAs. One nanomole of the RNA was renatured by heating at 95°C at 1 min, and then mixed with 10 µl Ni-NTA Magnetic Agarose Beads (QIAGEN) prefilled with mPrrp-FL in 1 ml binding buffer [0.5 M LiCl, 20 mM Tris–HCl (pH 7.5), 1 mM $MgCl_2$], and the mixtures were incubated on a rotator for 60 min at 4°C. After washing five times with binding buffer, the agarose resin with the RNA–protein complex was extracted with phenol/chloroform and the RNA in the aqueous phase was precipitated with ethanol. The selected RNA was reverse transcribed, and PCR amplification of the DNA product was performed using a one-tube RT–PCR kit (Amersham) under the following conditions: 30 min 42°C for reverse transcription, and 15 cycles of 30 s at 94°C, 30 s at 59°C, 5 s at 72°C for PCR amplification. The RT–PCR product was used for the next round of the selection procedure. After five rounds of selection, the RT–PCR product was subcloned into the pUC119 vector and sequenced.

Gel mobility shift assays

Gel mobility shift assays were performed with recombinant mPrrps and 5′-end labeled RNA probes in RNA-binding buffer [20 mM HEPES (pH 7.6), 3 mM $MgCl_2$, 40 mM KCl, 2 mM DTT, 5% glycerol]. Heterogeneous RNAs (10 pmol) obtained on each round of selection or RNAs cloned after five rounds of selection were 5′-end labeled with [γ-^{32}P]ATP and T4 polynucleotide kinase (New England Biolabs). Various amounts of recombinant mPrrp protein were incubated with 1000 c.p.m. of RNA probe (~10 fmol) for 15 min at room temperature in 20 µl of RNA-binding buffer containing 1 µg yeast tRNAs. For the competition experiments, unlabeled RNA was added before the addition of the labeled RNA. After incubation, the mixtures were immediately loaded onto 3.5% polyacrylamide gels (60:1) and fractionated by electrophoresis in 0.5× TBE. The gels were then dried and exposed to an Imaging plate (Fuji Film), and were visualized by a Bioimaging Analyzer, BAS-2000 (Fuji Film). The autoradiograms were quantitated by using MacBAS program (Fuji Film). The apparent dissociation constant (K_d) was estimated using Kaleida Graph software (Synergy Software).

Preparation of deletion and point mutants of S-13 RNA

For the preparation of deletion mutant RNAs of S-13, template cDNAs for *in vitro* RNA transcription were generated by PCR using S-13 cDNA as the template and the following pairs of primers: to obtain 3′ deletion mutants, the SELEX forward primer as a common forward primer, and 5′-CGG GAT CCC ATA GCC CGC AGC TAT AC-3′ (DM 1–73), 5′-CGG GAT CCC CGC AGC TAT ACT AAA CTA AGG-3′ (DM 1–67) and 5′-CGG GAT CCA CTA AAC TAA GGC CAC AAA CTA TT-3′ (DM 1–57) as reverse primers; to obtain 5′ deletion

mutants, the SELEX reverse primer as a common reverse primer, and 5′-GCG AAT TCT AAT ACG ACT CAC TAT AGG CAT AGC CAA ATA GTT TGT GGC-3′ (DM 26–89) and 5′-GCG AAT TCT AAT ACG ACT CAC TAT AGG CAA ATA GTT TGT GGC CTT AG-3′ (DM 32–89) as forward primers. After PCR amplification, the products were digested with EcoRI and BamHI, and then subcloned into the pUC119 vector and sequenced. A fragment from nucleotides 26 to 73 of S-13 RNA and its point mutants were obtained by direct *in vitro* transcription using the following oligonucleotides: 5′-TAA TAC GAC TCA CTA TAG GCA TAG CCA AAT AGT TTG TGG CCT TAG-3′ (sense); 5′-GAT CCC ATA GCC CGC AGC TAT ACT AAA CTA AGG CCA CAA ACT ATT TGG-3′ (antisense), and oligonucleotides with the corresponding nucleotide changes. These partial complementary oligonucleotides were annealed and filled in with *Taq* DNA polymerase (Promega), and then used for *in vitro* transcription.

RNase structural mapping

5′-end labeled RNAs (20 000 c.p.m.) were heat-denatured and then incubated in RNase digestion buffer [20 mM Tris–HCl (pH 7.0), 10 mM $MgCl_2$, 50 mM NaCl] with 5 μg yeast tRNAs (Sigma) at room temperature. After 30 min, 0.05 U of RNase T_1 (Ambion), 0.005 U of RNase V_1 (Ambion), or 1 U of mung bean nuclease (TaKaRa) was added, followed by incubation at 37°C for 5 min. The reactions were terminated by the addition of an equal volume of 9 M urea loading buffer, and samples were electrophoresed on a 12 or 20% polyacrylamide gel.

RESULTS

In vitro RNA selection of RNA ligands for mPrrp

To determine the RNA sequence for binding to mPrrp, we used an affinity elution-based RNA selection method (SELEX). Initially, we planned to use bacterially expressed His_6-tagged mPrrp for the selection of RNA–protein complexes. However, the His_6-Tagged mPrrp was extremely insoluble, and so we prepared a soluble form of mPrrp tagged with thioredoxin and His_6 (Figure 1A, mPrrp-FL). An initial RNA pool containing 50 nt random sequences was synthesized by *in vitro* transcription using a PCR-amplified oligonucleotide library as the template. The complexity of this initial RNA pool was estimated to be 10^{14}. The selection procedure was started by mixing 1 nmol of preabsorbed initial RNA pool with Ni-NTA Magnetic Agarose Beads prefilled with mPrrp-FL. After the binding reaction, the selected RNAs were reverse transcribed and the product cDNAs were amplified using the SELEX primer (see Materials and Methods for primer sequences), and the cDNAs were used again as templates to synthesize RNAs for the next round of the selection procedure.

To monitor the progression of RNA selection, RNA samples prepared after each round were subjected to gel mobility shift assay with mPrrp-2xRBD, which included the RNA-binding domains of mPrrp (Figure 1B). The RNA–protein complex was not detected when the initial RNA pool was incubated with mPrrp-2xRBD (Figure 1B, lane 1). With the progression of the selection round, the intensity of the RNA–protein complex increased and reached a plateau after the fifth round of RNA selection (Figure 1B, lanes 2–5), indicating that high-affinity RNA ligands for mPrrp-FL were sufficiently selected from the initial RNA pool. Moreover, the recombinant protein of the C-terminal proline-rich region of mPrrp did not give an RNA–protein complex with the RNA prepared after the fifth round (Figure 1B, lane 8). These results indicate that the RNA selection was indeed specific with respect to the RNA-binding domain of mPrrp.

Therefore, the selected cDNAs were subcloned into the pUC119 vector and sequenced. We then determined the sequences of 45 independent cDNA clones to identify the RNA consensus sequence that was conserved in these clones. In addition to 23 redundant clones carrying the same sequences, 22 unique sequences were obtained and are shown in Figure 1C. Comparison of these sequences revealed the well-conserved sequence element 'AAAUAG' (element 1, termed E1), which was found in 10 of the 22 clones, and single-base substitution variants within the three 5′ A residues of E1 (e.g. S-9, AGAUAG). This analysis also revealed another short conserved sequence, 'GUAG', which was found in 17 of the 22 clones. Three GUUAG sequences, one GUUUAG sequence and its single-base substitution variants of U residue (S-18 and S-29) were also observed, suggesting that $GU_{1-3}AG$ is another conserved sequence element (element 2, termed E2). We classified these sequences into four groups, Groups A–D (Figure 1C). Group A is the most abundant group derived from 15 clones, and the sequences contain both E1 and E2. Interestingly, the two conserved elements are located in the same order along the chain, E2 appearing at 10–20 nt downstream of E1. Group B sequences contain only a single E1. Group C sequences contain only E2, whereas S-14 contains four elements. Group D sequences contain no conserved element.

mPrrp binds RNAs that include both AAAUAG and $GU_{1-3}AG$

To determine whether or not the RNAs obtained by SELEX can interact with mPrrp with high affinity, representative RNAs from different groups were tested for binding to mPrrp-2xRBD by means of gel mobility shift assays. S-2, S-13 and S-52 RNAs belong to group A, and contain both the conserved elements. Gel mobility shift assays showed that S-2 and S-13 bound to the RNA-binding domain of mPrrp with high affinity (K_d, ∼43 and 56 nM, respectively), but S-52 did not (Figure 2A). The RNAs that belong to groups B (S-40) and C (S-31), each lack one of the conserved elements, and group D (S-27), without either conserved element, did not bind to mPrrp (data not shown). Because S-13 RNA was the highest affinity ligand for mPrrp among the examined RNAs, we next performed competitive binding assays to determine whether or not mPrrp bound specifically to S-13 RNA. About 10 fmol of ^{32}P-labeled S-13 RNA was incubated with 6 pmol of mPrrp (final, 300 nM) and a 10-, 100- or 1000-fold excess of unlabeled cold RNA, followed by gel shift analysis (Figure 2B). The intensities of the retarded bands representing the protein–RNA complex decreased on the addition of increasing amounts of unlabeled RNA containing the conserved elements as a specific competitor (Figure 2B; lanes 3–5). However, the intensities did not decrease on the addition of RNA that did not contain the conserved elements (Figure 2B; lanes 6–8).

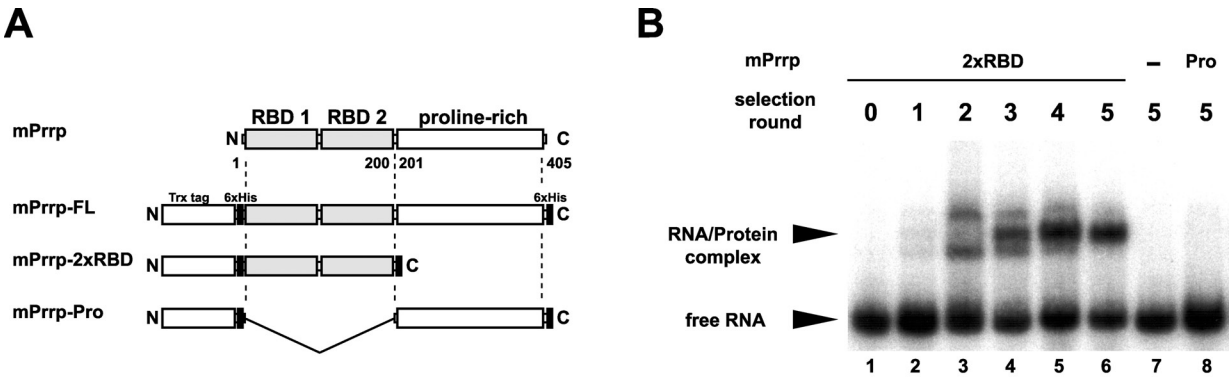

C

group	clone	sequence
A	S-2	CGAGUGCAACGCGACC**AAAUAG**GAUGGGG**GUUAG**GACCCGGGUCUUGCG
	S-9	GGCGGCC**AGAUAG**UCGGUGCACCG**GUAG**GGUGGACGGGUCGCCGGGGUGC
	S-12	g**aag**UAGUCGGCCUCGA**GUAG**CGGGGUGCUGGUUGGAGUCAGUUGGCGUGGG
	S-13	AUGAACAUAGCC**AAAUAG**UUUGUGGCCUUA**GUUUAG**UAUAGCUGCGGGC
	S-17	GACGCAUGCCGUC**AAAUAG**CUGGAUUGGUCGGGAGCGU**GUAGGUAG**CGG
	S-18	UCCAC**AGAUAG**UAUCAUAUCAACAA**GUAUAG**GGGUGAUGUGGGUGGGC
	S-19	**aagAUAG**GGACCGUGGUUA**GUAG**GACGAACGGGUUUGGUGAGGAUCACGUG
	S-24	GC**AAAUAG**UUUGGC**GUUAG**GAUGCUGGCCUUCGGGUUUCGGGGUUAUUGA
	S-26	CGGUCGGCAGC**AAAUAG**UAGGUUAUGCGAAG**GUUAG**AGCAAUAGCGGCUG
	S-28	**aagAUAG**UGCGCCGUCUGGGCCGGGUGACGU**GUAG**AGUUGAUUUCGUGGCGGC
	S-29	CAGACCACUC**AAAUAG**UUGUGAGCGUG**GAUAG**AGGCGCUUGGAGUUGG
	S-34	CC**AAGUAG**GUAGUGCGUUCUGGGACGGCG**GUAG**GGCGUGGGCGCUGCG
	S-35	AGGCGGC**AAAUAG**UCAGGGAGUAUAUUA**GUAG**GAGUCCCGGUCCCUC
	S-48	CGGUGUACAGGCC**AAAUAG**CGUUGUCGGCA**GUAG**GUCGGCGGGCCUAGC
	S-52	GAGUGUGGAGCAAGCGUUCA**AAAUAG**UGGGCCGGG**GUAG**CUGGUUGUG
B	S-11	GUCAUUCCAGUAGUGUUA**AAGUAG**GAAUUUAUCAGUCUGGUUGUCGUGCG
	S-30	GGCCC**GAAUAG**UGUUGGCUCAUUGGAGCGGGGUGGGUCGAACGAAGGGG
	S-40	CGCGUGGGGAGCUACGGC**AAAUAG**UCAGGUUCGAGCGGACCGGCCGUUG
C	S-14	GACUGUGUAAUCUCCCGUAU**GUAG**UUU**GUAG**UUU**GUAG**UU**GUAG**GGUGUC
	S-31	AGCUGUGGAGGCGACGCGCGGGGUCGACUAGCGGCCUCGGGG**GUAG**UGGU
	S-51	UGAUGGUCCCUUGUUUACUGCUUGGGCCUUAUGUGCAGGGA**GUAG**CACCU
D	S-27	CCAUUAGGGGAGCCUUGCAGCAGGUUGUCGGGAGGAAGUUCGGCUGCAG

Figure 1. *In vitro* selection of RNA ligands for mPrrp using random RNA pools. (**A**) Schematic representation of the domain structure of mPrrp protein and mutants used in this study. The full-length mPrrp (405 amino acids) contains both RBDs in the N-terminal region and a proline-rich region in the C-terminal region. The bacterially expressed full-length mPrrp (mPrrp-FL, 1–405 amino acids), RNA-binding domain (mPrrp-2xRBD, 1–201 amino acids), and proline-rich region (mPrrp-Pro, 201–405 amino acids) derivatives contain a thioredoxin-tag, and His-tags at the N- and C- terminals. (**B**) Confirmation of the progress of the RNA selection was performed by gel mobility shift assay. Ten femtomoles of RNA prepared from each round of selection was labeled with ^{32}P and incubated with 6 pmol mPrrp-2xRBD (final, 300 nM; lanes 1–6) or mPrrp-Pro (lane 8), and then the mixture was analyzed by electrophoresis. Free RNA probes and RNA–protein complexes are indicated by arrowheads. (**C**) The sequences of 22 unique clones obtained after five rounds of RNA selection are shown. The conserved sequence elements are indicated by hatched bold characters (E1) and underlined bold characters (E2). The individual sequences are classified into four groups: Group A containing both E1 and E2, Group B (E1 only), Group C (E2 only) and Group D (not containing any conserved elements). The sequences derived from the constant primer sequences are indicated in lower case characters.

These results indicate that S-13 RNA strongly and specifically binds to mPrrp.

Minimum RNA sequence of S-13 RNA contains two conserved elements

To determine the minimum region of S-13 RNA that is required for the efficient binding to mPrrp, we performed deletion mutant analysis of the RNA. 5′-end-labeled truncated RNAs were examined by means of gel mobility shift assays using mPrrp-2xRBD (Figure 3A). In the case of RNAs truncated from the 3′ end, DM 1–73 bound to mPrrp with high affinity (K_d, ~38 nM, Figure 3B; lanes 1–3), but DM 1–67 and DM 1–57 did not (Figure 3B; lanes 4–9). Similar analysis with the RNAs truncated from the 5′ end showed that DM 26–89 bound to mPrrp with high affinity (K_d, ~41 nM, Figure 3B; lanes 10–12), but DM 32–89 did not (Figure 3B; lanes 13–15). Next, we determined minimum RNA region for mPrrp binding. DM 26–73 RNA bound to mPrrp as strongly as the

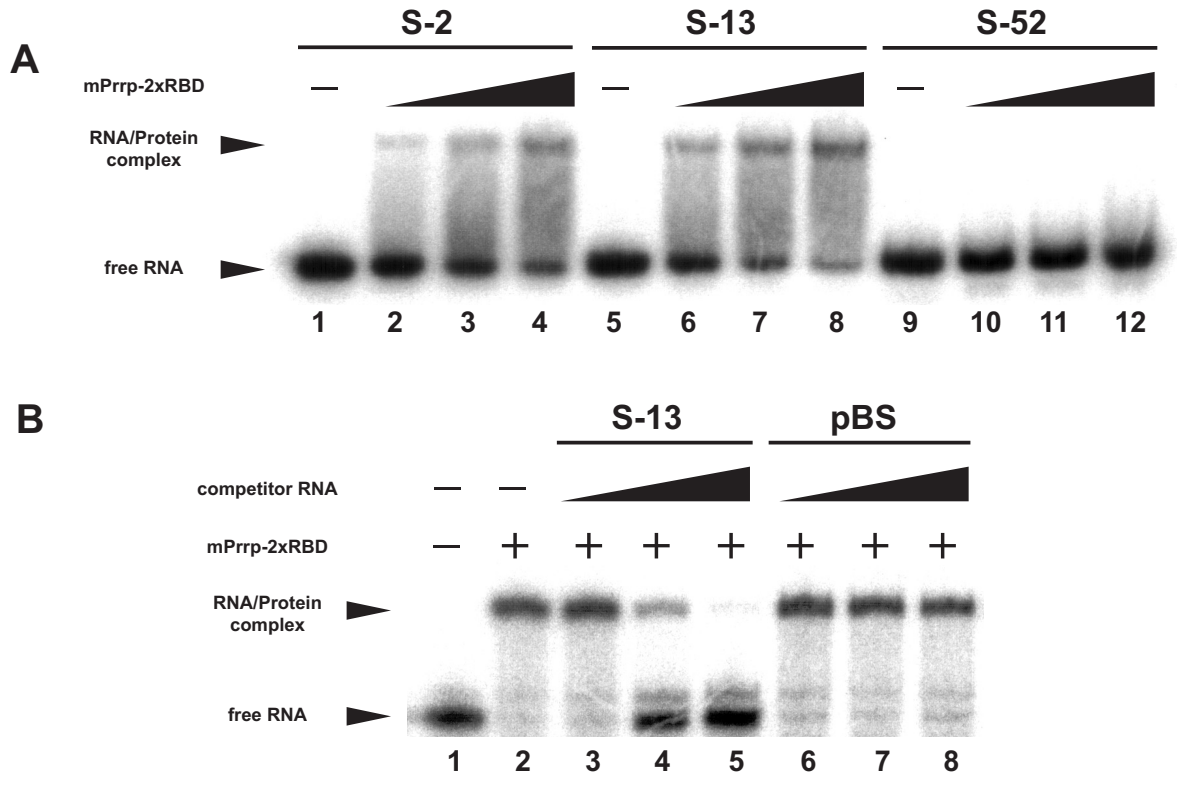

Figure 2. Binding experiments on several selected RNAs and mPrrp-2xRBD protein. (**A**) Gel mobility shift assay of mPrrp-2xRBD protein with several selected RNAs (S-2, lanes 1–4; S-13, lanes 5–8; and S-52, lanes 9–12). An aliquot of 10 fmol of ^{32}P-labeled RNAs (final, 0.5 nM) was incubated with various concentrations of mPrrp-2xRBD protein: 0 nM (lanes 1, 5 and 9), 50 nM (lanes 2, 6 and 10), 100 nM (lanes 3, 7 and 11) and 300 nM (lanes 4, 8 and 12), and the mixtures were run on non-denaturing polyacrylamide gels. (**B**) Competitive RNA-binding experiments involving unlabeled RNAs. Ten femtomoles (final, 0.5 nM) of ^{32}P-labeled S-13 RNA was incubated with mPrrp-2xRBD protein at a final concentration of 300 nM, and the following amounts of unlabeled competitor RNAs: 100 fmol (lanes 3 and 6), 1000 fmol (lanes 4 and 7) and 10 000 fmol (lanes 5 and 8). Free RNA probes and RNA–protein complexes are indicated by arrowheads. pBS RNA was transcribed from pBluescript SK(+) digested with XbaI.

full-length S-13 RNA (K_d, ~56 nM, Figure 3B; lanes 16–18). Therefore, we conclude that the region of S-13 RNA from nucleotide 26 to 73 is the minimum sequence for binding to mPrrp. The minimum RNA sequence contains both the conserved elements internally, suggesting the importance of these elements. In addition, we found that the flanking sequences of these elements, 8 nt upstream from E1 and 18 nt downstream from E2, were also required for mPrrp binding.

The AAAUAG and GUUUAG sequences are necessary for mPrrp binding

The minimum sequence of S-13 RNA required for mPrrp binding contains both E1 and E2, indicating that the sequences of these elements are important for binding to mPrrp. Next, to elucidate the importance of the primary sequences of the conserved elements, E1 and E2, we conducted a site-directed mutagenesis experiment for the S-13 RNA. Single point mutations were introduced at all nucleotides of the two conserved elements. Because Northwestern analysis in a previous study demonstrated that mPrrp preferably bound to Poly(A), (G) and (U), but did not interact with poly(C) *in vitro* (3), each residue in the conserved elements was substituted with a C residue. All point mutations in E1 almost completely abolished the interaction with mPrrp (Figure 4A). Point mutations in E2 generally had a drastic effect on binding affinity as well as those of E1, whereas mutants as to the second U (U52C) and the third U (U53C) retained binding affinity (K_d, ~55 and 75 nM, respectively, Figure 4B). These results reveal that both the conserved elements are indeed required for mPrrp binding, and an intact AAAUAG sequence is required for E1, but the sequence in E2 seems to be more tolerant as to the base specificity or U-stretch length.

The RNA ligands for mPrrp require an appropriate secondary structure containing E1 and E2

Deletion mutant analysis of S-13 RNA revealed that not only the sequences of the two conserved elements, but also the flanking sequences around these elements were required for efficient binding of S-13 RNA to mPrrp. These extra sequences are not conserved among selected RNAs, suggesting that these sequences contribute to binding to mPrrp by forming a specific structure. Therefore, we determined the secondary structure of S-13 RNA by means of RNase footprinting experiments using structure- or sequence-dependent RNases (RNase V_1, specific for RNA in helical and stacked regions; RNase T_1, specific for G in single-stranded RNAs; and mung bean nuclease, specific for RNA in single-stranded regions), in conjunction with secondary structure prediction using the Mfold program (11). The 5′-end-labeled full-length S-13 RNA was subjected to enzymatic probing under native

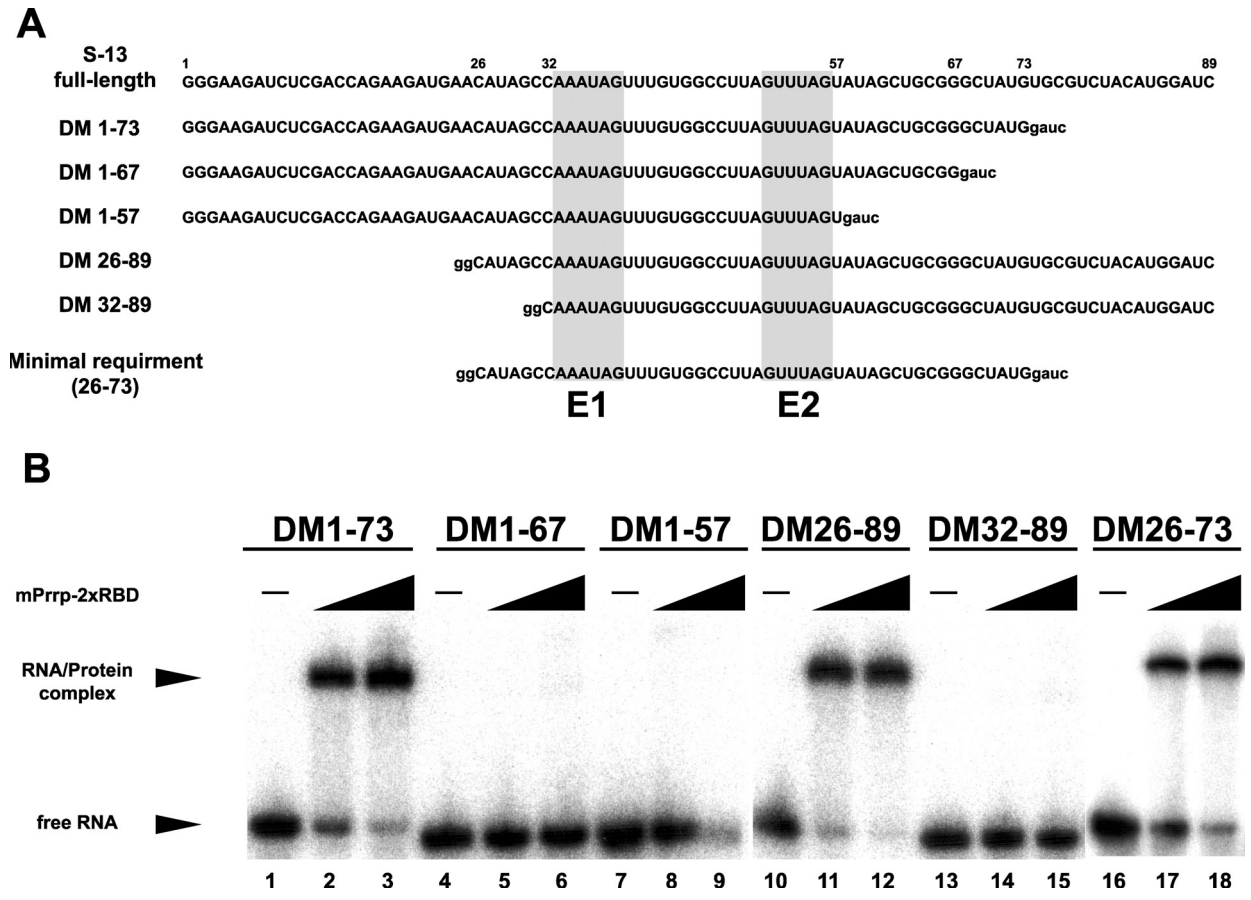

Figure 3. Minimum sequence requirement of S-13 RNA. (**A**) The sequences used for deletion mutant analysis of S-13 RNA are shown. The mutant names derive from the positions at the start and end of the full-length S-13 RNA. The minimum RNA sequence for binding to mPrrp is indicated at the bottom (positions 26–73). The lower case character sequence at 5′ terminal is derived from the sequence for transcription initiation by T7 RNA polymerase and the other one at the 3′ terminal is derived from the sequence of the restriction enzyme site (BamHI). (**B**) Gel mobility shift assay of mPrrp-2xRBD protein with deletion mutants. Ten femtomoles of ^{32}P-labeled RNAs (final, 0.5 nM) was incubated with various concentrations of mPrrp-2xRBD protein: 0 nM (lanes 1, 4, 7, 10, 13 and 16), 100 nM (lanes 2, 5, 8, 11, 14 and 17) and 300 nM (lanes 3, 6, 9, 12, 15 and 18), and the mixtures were run on non-denaturing polyacrylamide gels. Free RNA probes and RNA–protein complexes are indicated by arrowheads as in previous figures.

conditions (Figure 5A). Mung bean nuclease strongly cleaved nucleotides in two regions (nucleotides 34–40 and 50–57; Figure 5A, lane 5), and three G residues located in these regions (G38, G51 and G56) were strongly cleaved by RNase T_1 (Figure 5A, lane 2). These regions contain the 'AUAG' sequence of E1 and all nucleotides of E2, respectively, suggesting that both the conserved elements are mainly located in the single-stranded region. RNase V_1 cleaved in three regions (nucleotides 28–30, 32–35 and 46–48), but RNase T_1 did not cleave G30, G42, G44 and G45 efficiently (Figure 5A, lanes 2 and 4). These results suggest that these regions are located in double-stranded regions. These digestion patterns were mapped to the putative secondary structure model predicted with the Mfold program (Figure 5C). The predicted structure well corresponded to the digestion patterns with the RNases, however, the two A residues (A33 and A34) in a bulge loop (termed L1) indicated by Mfold were located in the region cleaved by RNase V_1. Because substitution of U39 to A and U40 to A did not change the digestion pattern with RNase V_1 (data not shown), the digestion with the region containing the two A residues might not be the result of Watson–Crick type base-pairing. Therefore, the essential part of S-13 RNA (nucleotides 26–73) forms two loop structures, one is a bulge loop (nucleotides 33–40) containing E1 and the other is a hairpin loop (nucleotides 51–56, termed L2) containing E2, and two long stem structures formed by the flanking sequences outside of the two conserved elements.

Among group A sequences containing both conserved elements, S-2 and S-13 bound to mPrrp, but S-52 did not (Figure 2A). The differences in binding affinity to mPrrp protein were thought to be due to the difference in the secondary structures of these RNAs. Therefore, RNase footprinting and computer-assisted secondary structures prediction were performed for S-2 and S-52 RNAs. The enzymatic probing of S-2 showed a very similar digestion pattern to that of S-13 RNA (electrophoresis data not shown). In the L1 region of S-2, interestingly, the two A residues of E1 were also located in the region cleaved by RNase V_1 (Figure 5D). The two nucleotides downstream of E1 of S-2, corresponding to the two U residues of E1 of S-13 RNA, were 'GA' residues, and the sequences are not conserved in other selected clones, supporting the observation for S-13 RNA that the cleavage near the two A residues of E1 is not the result of Watson–Crick type base-pairing. In the case of S-52 RNA, almost all of G residues

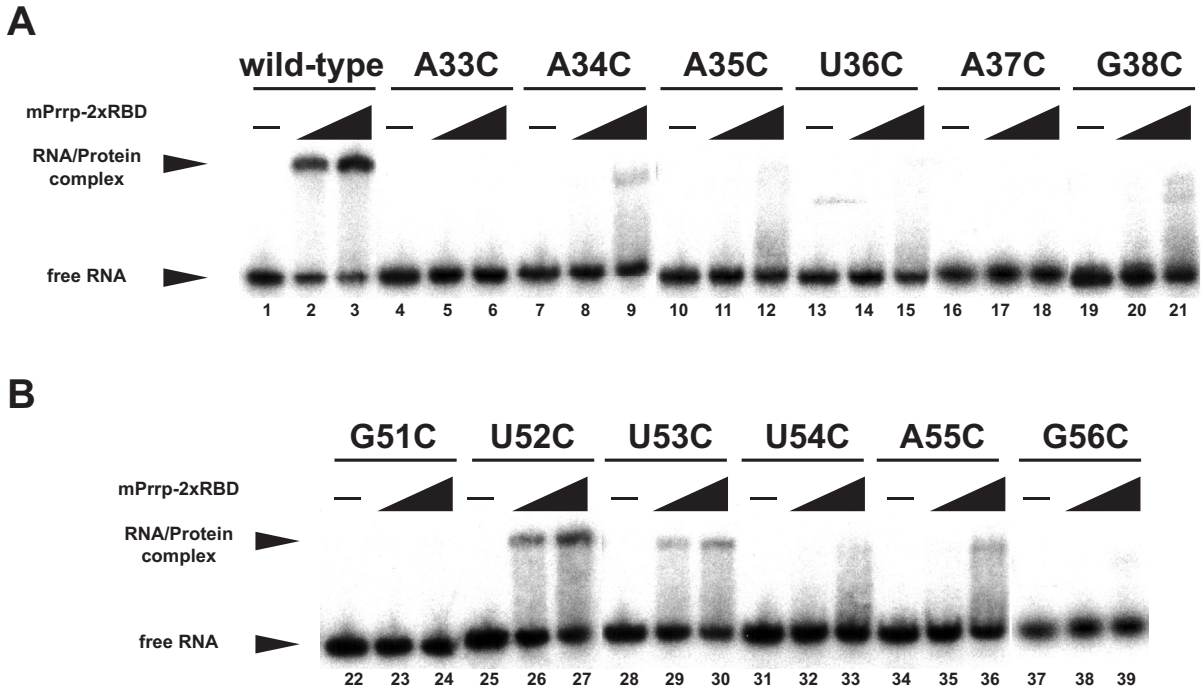

Figure 4. Point mutation analysis of the putative binding sites in S-13 RNA by gel mobility shift assay. Point mutations were introduced in to E1 (lanes 1–21) and E2 (lanes 22–39) in S-13 RNA. An aliquot of 10 fmol of ^{32}P-labeled RNAs (final, 0.5 nM) was incubated with various concentrations of mPrrp-2xRBD protein: 0 nM (lanes 1, 4, 7, 10, 13, 16, 19, 22, 25, 28, 31, 34 and 37), 100 nM (lanes 2, 5, 8, 11, 14, 17, 20, 23, 26, 29, 32, 35 and 38) and 300 nM (lanes 3, 6, 9, 12, 15, 18, 21, 24, 27, 30, 33, 36 and 39), and the mixtures were run on non-denaturing polyacrylamide gels. Free RNA probe and RNA–protein complexes are indicated by arrowheads as in previous figures.

were efficiently cleaved by RNase T1 (Figure 5B, lane 3), and many residues located in the regions upstream of E1 and downstream of E2 were cleaved by mung bean nuclease (Figure 5B, lane 5). These results indicate that S-52 RNA may not form a rigid structure. In addition, the predicted secondary structure by Mfold is not similar to those of S-2 and S-13 RNAs (Figure 5E). Therefore, the RNA ligands for mPrrp require the appropriate two loops and stem structures, and, in particular, L1 is not the normal bulge loop structure that is digested by RNase V_1 without canonical base-pairing.

To determine whether or not this stem–loop structure contributes to the binding ability of S-13 RNA to mPrrp, we compared the secondary structures of the deletion mutants and the wild-type S-13 RNA. First, we compared the secondary structures of 3′-truncated RNAs with that of the wild-type S-13 RNA (Figure 6A). In the L1 of DM 1–67 and DM 1–57 (not bound to mPrrp), no remarkable differences were observed in the digestion patterns between the wild-type and deleted RNAs with either RNase V_1 or mung bean nuclease. However, the digestion pattern of L2 with mung bean nuclease was different from those of wild-type and DM 1–73 RNA, both of which bound to mPrrp (Figure 6A, lanes 2–8 versus 9–14). Mung bean nuclease strongly cleaved the nucleotides in L2 of the wild-type and DM 1–73 RNA, but did not cleave those of DM 1–67 or DM 1–57 RNA. The digestion pattern of DM 1–67 was mapped on the putative secondary structure model predicted with the Mfold program, as shown in Figure 6B. Next, we compared the secondary structures of 5′-truncated RNAs with that of the full-length RNA (Figure 6C and D). The digestion patterns of the 3′ portions of DM 26–89 and DM 32–89 RNAs showed the same pattern as that of the wild-type RNA (not shown). But, the digestion pattern of L1 of DM 32–89 RNA was different from those of the full-length and DM 26–89 RNA. In E1 of DM 26–89, RNase V_1 cleaved near A33 and A34, and the region containing A35–G38 were cleaved by mung bean nuclease, whereas all nucleotides of E1 of DM 32–89 were cleaved by mung bean nuclease, but none by RNase V_1 (Figure 6C, lanes 4 and 5 versus 9 and 10). These digestion patterns were mapped on the putative secondary structure models predicted with the Mfold program, as shown in Figure 6D. These models suggest that the stem structure formed by two extra strands outside of the two conserved elements, i.e. the nucleotides from C26 to C32 and from G67 to G73, are disrupted in the mutant RNAs, which do not bind mPrrp, and indicate that there is a good correlation between the competence of an RNA ligand and the existence of two loop structures.

DISCUSSION

In this study, *in vitro* RNA selection experiment was performed to determine the target RNA-binding sequence of mPrrp. Sequence analysis revealed that many clones obtained on selection contained two conserved sequences elements, AAAUAG (E1) and $GU_{1-3}AG$ (E2), separated by 10–20 nt. All single substitutions in the two conserved sequence elements of S-13 RNA decreased the binding to mPrrp, indicating that both these elements might be critical for the interaction with mPrrp. We also showed that the RNA secondary structure

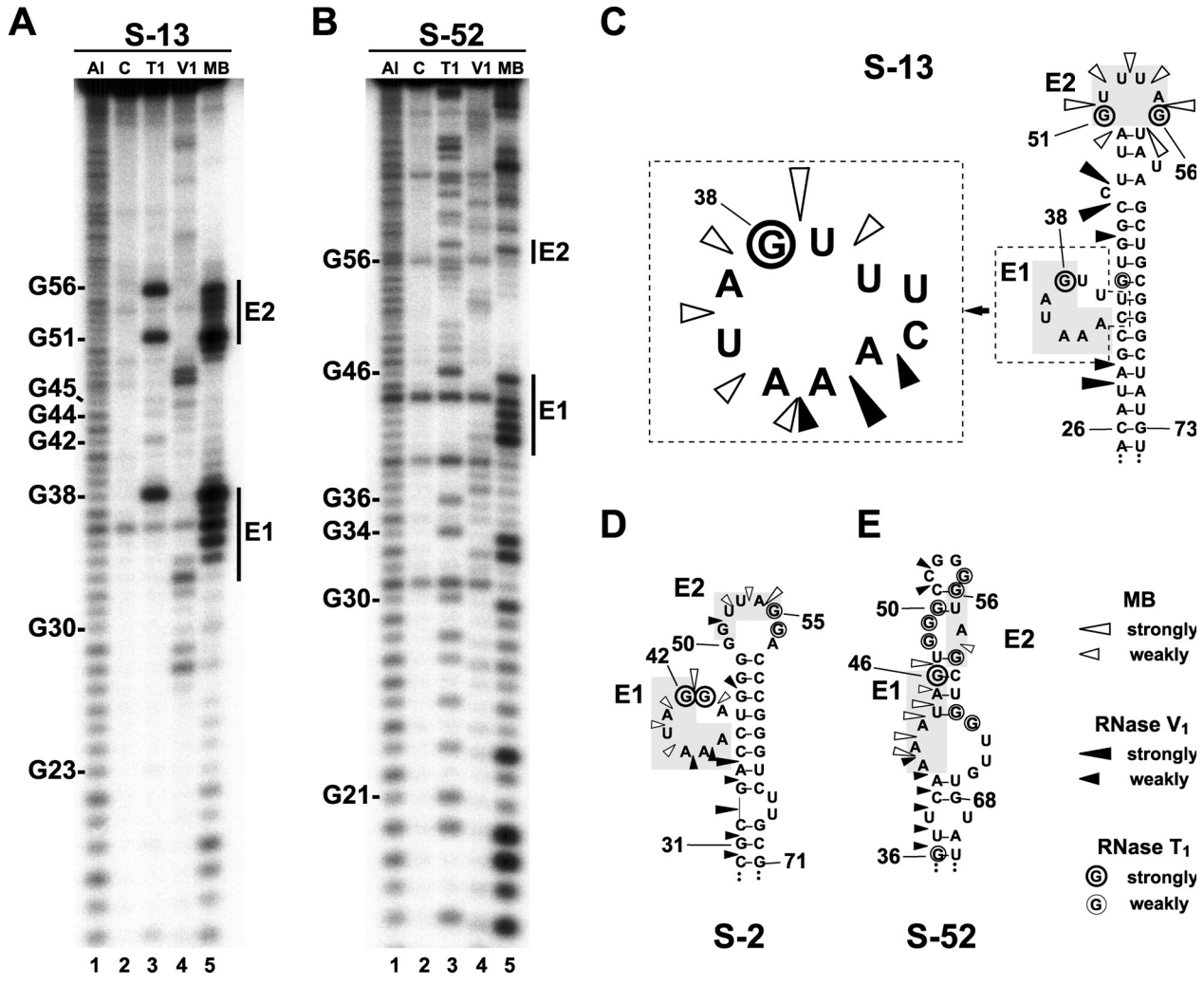

Figure 5. Secondary structure analysis of the selected RNAs. 5′-^{32}P-labeled full-length S-13 RNA (**A**) and S-52 RNA (**B**) were subjected to partial digestion with sequence- or structure-dependent nucleases, and then run on 12% polyacrylamide sequencing gels. (A and B): Al (lane 1), alkaline hydrolysis products as size marker; C (lanes 2), untreated RNAs as a control; T1 (lane 3), RNase T_1; V_1 (lanes 4), RNase V_1; and MB (lanes 5), mung bean nuclease. The secondary structure models superimposed with RNase digestion results, S-13 (**C**), S-2 (**D**) and S-52 (**E**), are shown. Cleavage sites for RNase V_1 and mung bean nuclease are indicated by filled and open arrowheads, respectively, and relative cleavage intensities are indicated. The G residues cleaved by RNase T1 are indicated by open circle, and relative cleavage intensities are shown.

consisting of two conserved elements and the flanking sequences were critical for the mPrrp binding.

Interestingly, both the conserved sequence elements required for mPrrp binding contained the common UAG sequence. Three proteins that bind RNA sequences containing the UAG core sequence have been reported: hnRNP A1 binds to UAGGGA/U (12), hnRNP D to UUAG (13), and Musashi1 to (G/A)U_{1-3}AGU (8). Two RBDs of mPrrp exhibit high sequence homology (RBD1: 46–55% identity, 67–71% similarity; RBD2 38–41% identity, 60–66% similarity) to RBDs of these proteins. These amino acid sequence homologies are in good agreement with the target RNA sequences of mPrrp that contain the UAG core sequence. But, mPrrp requires two consensus sequences for binding a target RNA.

It is known that, in addition to a primary structure, an ordered secondary structure is required for a target RNA of some RNA-binding proteins. U1a binds to the AUUGCAC sequence located in the 5′-half of a 10 nt loop closed by a 5 bp stem (14), Nucleolin binds to the UCCCGA sequence in an 8 nt loop closed by a 4 bp stem (15). The binding affinity of these ligands decreases with disruption of the stem or alteration of the loop length (15–17), indicating that these RNA-binding proteins require both the primary structure and the strict secondary structure of the binding site. RNase footprinting experiments and secondary structure predictions of S-13 RNA and deletion mutants of it revealed that mPrrp also requires a specific secondary structure of the RNA ligand for the binding. The RNA ligand for mPrrp has two loop structures (L1 and L2), but their structural properties should be different from each other.

The secondary structure of L1 was predicted to be a bulge loop structure with the Mfold program, but in the RNase footprinting experiments, the regions containing the two A residues of L1 in S-13 and S-2 RNAs were commonly digested by RNase V_1. In the case of S-13, the base-pairing partner of these A residues was not the two U residues located in the

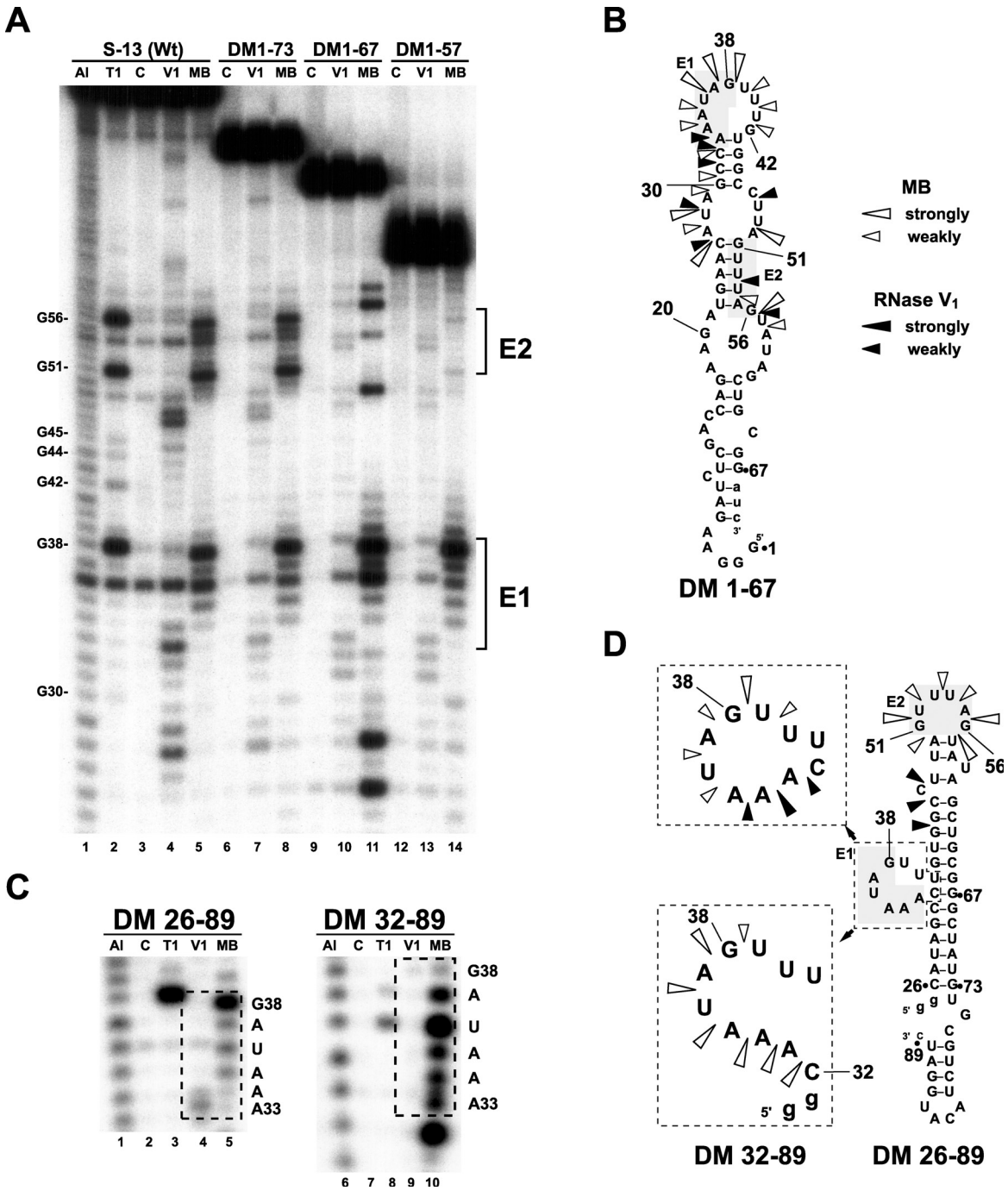

Figure 6. Secondary structure comparison of full-length S-13 RNA and its deletion mutants. 5′-^{32}P-labeled full-length S-13 RNA and its truncated, from the 3′-end (**A**) or from the 5′-end (**C**), mutants were subjected to partial digestion with sequence- or structure-dependent nucleases, and then run on 12 or 20% polyacrylamide sequencing gels, respectively. Al [lane 1 in (A); lanes 1 and 6 in (C)], with alkaline hydrolysis products as markers; T1 [lane 2 in (A); lanes 3 and 8 in (C)], RNase T_1; C [lanes 3, 6, 9 and 12 in (A); lanes 2 and 7 in (C)], untreated RNAs as a control; V_1 [lanes 4, 7, 10 and 13 in (A); lanes 4 and 9 in (C)], RNase V_1; and MB [lanes 5, 8, 11 and 14 in (A); lanes 5 and 10 in (C)], mung bean nuclease. The secondary structure models mapped with RNase digestion results, DM 1–67 (**B**), and DM 26–89 and 32–89 (**D**), are shown. Cleavage sites for RNase V_1 and mung bean nuclease are indicated by filled and open arrowheads, respectively, relative cleavage intensities are shown. The nucleotide positions of the mutants are numbered according to full-length S-13 RNA. The two G residues at the 5′ end of the RNAs required for transcription by T7 RNA polymerase and additional sequences of 3′ end restriction enzyme sites (BamHI) are indicated in lower case characters.

3′-portion of L1, and the sequences were not conserved in other selected clones. It would appear that there is no Watson–Crick type base-pairing in this region. RNase V_1 does not bind in the groove of a helix but a sugar phosphate backbone, showing that the activity does not always require hydrogen bonding (18). Both the A residues and the residues in the 3′-portion of L1 seem to be close to each other, therefore, this bulge loop region may form a stem–loop-like structure without canonical base-pairing, and these two A residues may result in a substrate for RNase V_1. Moreover, the predicted

bulge loop in both S-13 and S-2 consists of 8 nt, suggesting that the loop containing E1 requires rigorous restriction of the structure for mPrrp binding. On the other hand, L2 (containing E2) of S-13 and S-2 is located in a hairpin loop structure. The loop lengths of L2 in S13 and S-2 are 6 and 8 nt, respectively. The lengths of the U-stretch of E2 in other group A sequences are in the range of one to three. These observations suggest that the loop length of L2 can be varied for mPrrp binding. Point mutation experiments on E1 and E2 demonstrated that mPrrp exhibited high sequence specificity for E1, but was relatively tolerant as to E2. In conclusion, mPrrp recognizes two loop structures possessing different properties; L1 is constrained by both the sequence and secondary structure, and L2 exhibits flexible sequence specificity and a normal hairpin conformation containing E2.

The amino acid sequence identities of the two RBDs (RBD1: 11–83 amino acids, RBD2: 113–185 amino acids, mPrrp) of mouse and *Xenopus* Prrp are 100% (RBD1) and 96% (RBD2), indicating that the RNA sequences recognized by mouse and *Xenopus* Prrp should be similar to each other. Zhao *et al*. showed by immunoprecipitation assay that *Xenopus* Prrp bound Vg1 mRNA and other localized mRNAs (An1, An3 and VegT) in *Xenopus* oocytes (4). Vg1 and VegT mRNAs are transported to the vegetal hemisphere of *Xenopus* oocytes using the late pathway, while An1 and An3 mRNAs are transported to the animal hemisphere (19–21). In the 3′-UTR of these mRNAs, we found several E1 and E2 sequences revealed in this study (Table 1). The mRNAs encoding VegT and An1 contain an intact E1 (AAAUAG) sequence in the 3′-UTR, and Vg1 mRNA contains CAAUAG and UAAUAG, sequences with a one base substitution in the E1 sequence. These mRNAs also contain several E2 ($GU_{1–3}AG$) sequences in the 3′-UTR. In addition to these mRNAs, 3′-UTRs of *Xpat* and *Xvelo1*, which are essential for localization of the mRNA to the vegetal hemisphere using the late pathway in *Xenopus* oocytes (24,25), also contain intact E1 and E2 sequences in the 3′-UTR. According to these observations, it is highly possible that the mRNAs that bind to *Xenopus* Prrp *in vivo* contain both E1 and E2 sequences in the 3′-UTR, as in the case of mouse Prrp shown here.

mPrrp was first found as Daz associated protein 1 (DAZAP1) by yeast two-hybrid screening, and interacts with both DAZ and DAZL *in vitro* (3). Dazl proteins are assumed to play various roles in germ cell differentiation (26). In mouse spermatogenesis, Dazl protein is detected in spermatogonia to spermatocytes and its subcellular localization is mainly in the cytoplasm (26,27). On the other hand, mPrrp is not detected in spermatogonia but in the nuclei of late pachytene spermatocytes and round spermatids, and in the cytoplasm of elongating spermatids [(6), Kurihara *et al*., in press]. These immunohistochemical findings show that mPrrp and Dazl might not be colocalized during spermatogenesis, indicating that there is no functional interaction between mPrrp and mDazl. In fact, the putative target mRNA of Dazl, Cdc25C mRNA [determined from testis cDNA on SELEX; (28)] does not contain either E1 or E2, and Tpx-1 and Cdc25A mRNAs [determined by the SNAAP method, (29)] contain only E2, which is not enough for binding to mPrrp, as reported here. Therefore, mPrrp and mDazl seem to control different target mRNAs from different functional aspects.

The anchoring of localized mRNAs is the mechanism for retaining messenger ribonucleoprotein (mRNP) particles transiently in cortical microfilaments, and microfilament-associated proteins mediate this mechanism (30,31). *Xenopus* Prrp associates with both profilin and the EVH1 domain of Mena (4). Profilin is an actin-binding protein, which is thought to regulate actin polymerization (32), and Mena is localized in focal adhesions and in cell surface protrusions where the actin cytoskeleton is actively reorganized (33). Therefore, it is likely that Prrp mediates the anchoring of the Vg1 mRNP along the vegetal cortex by binding to profilin and Mena (4). The consensus amino acid sequence for profilin binding is GPPPP (34), and that for Mena binding is FPPPP (35). These amino acid sequences are well conserved in the proline-rich regions of Prrp in *Xenopus*, mouse and human, suggesting that the anchoring of the mRNA to cortical microfilaments may be a common function of the Prrp family. We confirmed that mPrrp bound to profilin III, which is specifically expressed in haploid spermatids [(36), Y. Kurihara, unpublished data].

Table 1. The locations of E1 and E2 in *Xenopus* mRNAs

Gene	Accession no.	Localization	Sequence and location[d]		Reference
			E1	E2	
Vgl	M18055	Vegetal	UAAUAG (1309 and 1788) CAAUAG (1885)	GUAG (1265, 1340, 1853, 1895 and 2250) GUUAG (1575 and 1582)	(22)
VegT	U59483	Vegetal	AAAUAG (2511)	GUAG (1643 and 2407)	(20)
Anla[a]	L08474	Animal	AAAUAG (2524)	GUAG (2744) GUUAG (2490 and 2708)	(23)
Anlb[a]	L08475	Animal	AAAUAG (2445)	GUAG (2689)	(23)
An3[b]		Animal	3′-UTR is not known		(23)
Xpat[c]	AJ002384	Vegetal	AAAUAG (3262 and 3799)	GUAG (1234, 1579, 1811, 2149, 2396, 2596, 3043, 3062, 3184, 3364, 3504 and 3693) GUUAG (1143, 2220 and 3180)	(24)
Xvelo1	AY280864	Vegetal	AAAUAG (2524 and 2598)	not identified	(25)

[a]Zhao *et al*. simply reported these genes as 'An1', but two An1 mRNA isoforms have been reported. Both the mRNAs are localized to the animal hemisphere of oocytes.
[b]The 3′-UTR of An3 mRNA is not registered with GenBank.
[c]There has been no report of Xpat mRNA binding to Prrp, but the 3′-UTR is essential for the localization of the mRNA to the vegetal hemisphere.
[d]The numbers of the locations are in accordance with those in GenBank.

Because of the translocation of mPrrp from the nucleus to the cytoplasm in elongating spermatids, mPrrp can be recruited to the site of actin polymerization through association with actin regulatory proteins. Therefore, we expected that mPrrp might be involved in the transport and anchoring of the mRNAs that encode proteins for actin metabolism.

ACKNOWLEDGEMENTS

This work was supported in part by a Grant-in-Aid from the Ministry of Education, Sports, Culture, Science and Technology of Japan (MEXT). Funding to pay the Open Access publication charges for this article was provided by Ministry of Education, Culture, Sports, Science and Technology.

REFERENCES

1. Hecht,N.B. (1998) Molecular mechanisms of male germ cell differentiation. *Bioessays*, **20**, 555–561.
2. Steger,K. (2001) Haploid spermatids exhibit translationally repressed mRNAs. *Anat. Embryol. (Berl.)*, **203**, 323–334.
3. Tsui,S., Dai,T., Roettger,S., Schempp,W., Salido,E.C. and Yen,P.H. (2000) Identification of two novel proteins that interact with germ-cell-specific RNA-binding proteins DAZ and DAZL1. *Genomics*, **65**, 266–273.
4. Zhao,W.M., Jiang,C., Kroll,T.T. and Huber,P.W. (2001) A proline-rich protein binds to the localization element of *Xenopus* Vg1 mRNA and to ligands involved in actin polymerization. *EMBO J.*, **20**, 2315–2325.
5. Mowry,K.L. and Melton,D.A. (1992) Vegetal messenger RNA localization directed by a 340-nt RNA sequence element in *Xenopus* oocytes. *Science*, **255**, 991–994.
6. Vera,Y., Dai,T., Hikim,A.P., Lue,Y., Salido,E.C., Swerdloff,R.S. and Yen,P.H. (2002) Deleted in azoospermia associated protein 1 shuttles between nucleus and cytoplasm during normal germ cell maturation. *J. Androl.*, **23**, 622–628.
7. Cho,Y.S., Chennathukuzhi,V.M., Handel,M.A., Eppig,J. and Hecht,N.B. (2004) The relative levels of translin-associated factor X (TRAX) and testis brain RNA-binding protein determine their nucleocytoplasmic distribution in male germ cells. *J. Biol. Chem.*, **279**, 31514–31523.
8. Imai,T., Tokunaga,A., Yoshida,T., Hashimoto,M., Mikoshiba,K., Weinmaster,G., Nakafuku,M. and Okano,H. (2001) The neural RNA-binding protein Musashi1 translationally regulates mammalian *numb* gene expression by interacting with its mRNA. *Mol. Cell. Biol.*, **21**, 3888–3900.
9. Buckanovich,R.J. and Darnell,R.B. (1997) The neuronal RNA binding protein Nova-1 recognizes specific RNA targets *in vitro* and *in vivo*. *Mol. Cell. Biol.*, **17**, 3194–3201.
10. Tanaka,Y., Hori,T., Tagaya,M., Sakamoto,T., Kurihara,Y., Katahira,M. and Uesugi,S. (2002) Imino proton NMR analysis of HDV ribozymes: nested double pseudoknot structure and Mg2 ion-binding site close to the catalytic core in solution. *Nucleic Acids Res.*, **30**, 766–774.
11. Zuker,M. (1989) On finding all suboptimal foldings of an RNA molecule. *Science*, **244**, 48–52.
12. Burd,C.G. and Dreyfuss,G. (1994) RNA binding specificity of hnRNP A1: significance of hnRNP A1 high-affinity binding sites in pre-mRNA splicing. *EMBO J.*, **13**, 1197–1204.
13. Kajita,Y., Nakayama,J., Aizawa,M. and Ishikawa,F. (1995) The UUAG-specific RNA binding protein, heterogeneous nuclear ribonucleoprotein D0. Common modular structure and binding properties of the 2xRBD-Gly family. *J. Biol. Chem.*, **270**, 22167–22175.
14. Tsai,D.E., Harper,D.S. and Keene,J.D. (1991) U1-snRNP-A protein selects a ten nucleotide consensus sequence from a degenerate RNA pool presented in various structural contexts. *Nucleic Acids Res.*, **19**, 4931–4936.
15. Ghisolfi-Nieto,L., Joseph,G., Puvion-Dutilleul,F., Amalric,F. and Bouvet,P. (1996) Nucleolin is a sequence-specific RNA-binding protein: characterization of targets on pre-ribosomal RNA. *J. Mol. Biol.*, **260**, 34–53.
16. Scherly,D., Boelens,W., van Venrooij,W.J., Dathan,N.A., Hamm,J. and Mattaj,I.W. (1989) Identification of the RNA binding segment of human U1 A protein and definition of its binding site on U1 snRNA. *EMBO J.*, **8**, 4163–4170.
17. Scherly,D., Boelens,W., Dathan,N.A., van Venrooij,W.J. and Mattaj,I.W. (1990) Major determinants of the specificity of interaction between small nuclear ribonucleoproteins U1A and U2B″ and their cognate RNAs. *Nature*, **345**, 502–506.
18. Lowman,H.B. and Draper,D.E. (1986) On the recognition of helical RNA by cobra venom V_1 nuclease. *J. Biol. Chem.*, **261**, 5396–5403.
19. Melton,D.A. (1987) Translocation of a localized maternal mRNA to the vegetal pole of *Xenopus* oocytes. *Nature*, **328**, 80–82.
20. Zhang,J. and King,M.L. (1996) *Xenopus* VegT RNA is localized to the vegetal cortex during oogenesis and encodes a novel T-box transcription factor involved in mesodermal patterning. *Development*, **122**, 4119–4129.
21. Rebagliati,M.R., Weeks,D.L., Harvey,R.P. and Melton,D.A. (1985) Identification and cloning of localized maternal RNAs from *Xenopus* eggs. *Cell*, **42**, 769–777.
22. Weeks,D.L. and Melton,D.A. (1987) A maternal mRNA localized to the vegetal hemisphere in *Xenopus* eggs codes for a growth factor related to TGF-beta. *Cell*, **51**, 861–867.
23. Linnen,J.M., Bailey,C.P. and Weeks,D.L. (1993) Two related localized mRNAs from *Xenopus laevis* encode ubiquitin-like fusion proteins. *Gene*, **128**, 181–188.
24. Hudson,C. and Woodland,H.R. (1998) *Xpat*, a gene expressed specifically in germ plasm and primordial germ cells of *Xenopus laevis*. *Mech. Dev.*, **73**, 159–168.
25. Claußen,M. and Pieler,T. (2004) Xvelo1 uses a novel 75-nucleotide signal sequence that drives vegetal localization along the late pathway in Xenopus oocytes. *Dev. Biol.*, **266**, 270–284.
26. Ruggiu,M., Speed,R., Taggart,M., McKay,S.J., Kilanowski,F., Saunders,P., Dorin,J. and Cooke,H.J. (1997) The mouse *Dazla* gene encodes a cytoplasmic protein essential for gametogenesis. *Nature*, **389**, 73–77.
27. Reijo,R.A., Dorfman,D.M., Slee,R., Renshaw,A.A., Loughlin,K.R., Cooke,H. and Page,D.C. (2000) DAZ family proteins exist throughout male germ cell development and transit from nucleus to cytoplasm at meiosis in humans and mice. *Biol. Reprod.*, **63**, 1490–1496.
28. Venables,J.P., Ruggiu,M. and Cooke,H.J. (2001) The RNA-binding specificity of the mouse Dazl protein. *Nucleic Acids Res.*, **29**, 2479–2483.
29. Jiao,X., Trifillis,P. and Kiledjian,M. (2002) Identification of target messenger RNA substrates for the murine deleted in azoospermia-like RNA-binding protein. *Biol. Reprod.*, **66**, 475–485.
30. Löpez de Heredia,M. and Jansen,R.P. (2004) mRNA localization and the cytoskeleton. *Curr. Opin. Cell Biol.*, **16**, 80–85.
31. Jansen,R.P. (1999) RNA-cytoskeletal associations. *FASEB J.*, **13**, 455–466.
32. Pollard,T.D. and Cooper,J.A. (1984) Quantitative analysis of the effect of *Acanthamoeba* profilin on actin filament nucleation and elongation. *Biochemistry*, **23**, 6631–6641.
33. Gertler,F.B., Niebuhr,K., Reinhard,M., Wehland,J. and Soriano,P. (1996) Mena, a relative of VASP and *Drosophila* Enabled, is implicated in the control of microfilament dynamics. *Cell*, **87**, 227–239.
34. Reinhard,M., Giehl,K., Abel,K., Haffner,C., Jarchau,T., Hoppe,V., Jockusch,B.M. and Walter,U. (1995) The proline-rich focal adhesion and microfilament protein VASP is a ligand for profilins. *EMBO J.*, **14**, 1583–1589.
35. Niebuhr,K., Ebel,F., Frank,R., Reinhard,M., Domann,E., Carl,U.D., Walter,U., Gertler,F.B., Wehland,J. and Chakraborty,T. (1997) A novel proline-rich motif present in ActA of *Listeria monocytogenes* and cytoskeletal proteins is the ligand for the EVH1 domain, a protein module present in the Ena/VASP family. *EMBO J.*, **16**, 5433–5444.
36. Braun,A., Aszódi,A., Hellebrand,H., Berna,A., Fässler,R. and Brandau,O. (2002) Genomic organization of *profilin-III* and evidence for a transcript expressed exclusively in testis. *Gene*, **283**, 219–225.